

# Emergent topological superconductivity at nematic domain wall of FeSe

Kyungmin Lee<sup>1</sup> and Eun-Ah Kim<sup>2</sup>

<sup>1</sup>*Department of Physics, The Ohio State University, Columbus, OH 43210, USA*

<sup>2</sup>*Department of Physics, Cornell University, Ithaca, New York 14853, USA*

(Dated: February 14, 2017)

One dimensional hybrid systems play an important role in the search for topological superconductivity. Nevertheless, all one dimensional hybrid systems so far have been externally defined. Here we show that one-dimensional domain wall in a nematic superconductor can serve as an emergent hybrid system in the presence of spin-orbit coupling. As a concrete setting we study the domain wall between nematic domains in FeSe, which is well established to be a nematic superconductor. We first show on the symmetry grounds that spin-triplet pairing can be induced at the domain wall by constructing a Ginzburg-Landau theory. We then demonstrate using Bogoliubov-de Gennes approach that such nematic domain wall supports zero energy bound states which would satisfy Majorana condition. Well-known existence of these domain walls at relatively high temperatures, which can in principle be located and investigated with scanning tunneling microscopy, presents new opportunities for a search for realization of Majorana bound states.

The realization that one-dimensional hybrid systems with spin-orbit coupling (SOC) [1, 2] or magnetism [3] can offer a new arena for topological superconductivity [see Ref. 4 and references therein] has led to renewed interest in one-dimensional superconductors. Moreover, broader appreciation of edge state properties of Dirac systems such as Weyl semimetal [5, 6], graphene [7], and nodal superconductors including a  $d$ -wave superconductor [8, 9] have emerged. Unfortunately, however, most of these systems require rather special conditions operating at extremely low temperatures. On the other hand, little attention has been paid to the fact that a domain wall in a superconductor with additional  $\mathbb{Z}_2$  symmetry breaking could form a new type of hybrid systems, although nematic order in superconducting phase is common [10, 11]. In iron-based superconductors, in particular, robust signatures of nematic phase transition has been detected and imaged [12, 13]. Boundaries between nematic domains, embedded in a spin-orbit coupled system, provide a new possibility towards realizing a novel one-dimensional superconductor. Motivated by this, we consider a new emergent hybrid situation of nematic domain wall in FeSe.

FeSe has generated much interest as a superconductor which exhibits nematicity without additional complication from magnetic order [14, 15]. Through real space probes, boundaries between two such nematic domains have been observed [16–18]. In this letter, we study the structure of superconducting pairing at nematic domain walls using symmetry analysis, and argue that spin-triplet pairing can be induced through spin-orbit coupling. Furthermore, we show, through Bogoliubov-de Gennes approach, that the ends of domain walls can support zero energy bound states. We also remark on the connection between our results and the recent works on the edge states of nodal superconductor [19, 20].

The superconducting gap structure of FeSe is still an unsettled issue. The two most widely discussed pair-

symmetry operation	tetragonal phase	orthorhombic phase	domain wall [ $1\bar{1}0$ ]
$2C_4$	o	×	×
$C_2$	o	o	×
$2\sigma_v$	o	o	×
$\sigma_d(x-y)$	o	×	o
$\sigma_d(x+y)$	o	×	×
point group	$C_{4v}$	$C_{2v}$	$C_s$

TABLE I. Point group symmetries in different phases. o and × respectively denote good and broken symmetry operations. The linear polynomial  $p$  in  $\sigma_d(p)$  defines the mirror plane by  $p = 0$ .

ing symmetries of iron-based superconductors are  $s$ -wave and  $d_{x^2-y^2}$ -wave [21]. In the tetragonal phase of FeSe, the point group symmetry on a surface of bulk material or of a single layer grown on a substrate is  $C_{4v}$ , and  $s$ - and  $d_{x^2-y^2}$ -wave belong to different representations of the point group ( $A_1$  and  $B_1$ , respectively) and hence the spin-singlet pairing is either purely  $s$ -wave or purely  $d_{x^2-y^2}$ -wave. However, in the orthorhombic phase ( $a \neq b$  and  $\gamma = 90^\circ$ , where  $a$  and  $b$  are the lengths of the lattice vectors and  $\gamma$  is the angle between them) the four-fold rotation ( $C_4$ ) and diagonal mirror reflection ( $\sigma_d$ ) symmetries are broken, resulting in  $C_{2v}$  as the reduced point group symmetry [see Tab. I]. In  $C_{2v}$ ,  $s$ -wave and  $d_{x^2-y^2}$ -wave are no longer distinguished, while other representations ( $A_2$ ,  $B_2$ , and  $E$ ) of  $C_{4v}$  stay symmetry-distinct from them. The pairing gap in the nematic phase therefore is a mixture of  $s$ -wave and  $d_{x^2-y^2}$ -wave. Within a Ginzburg-Landau (GL) theory, this mixing is described by

$$\mathcal{L}_{s-d} = \eta s^* d_{x^2-y^2} + \text{c.c.} \quad (1)$$

where  $\eta$  is a real field representing the strength of nematicity, and  $s$  and  $d_{x^2-y^2}$  are the pairing order param-

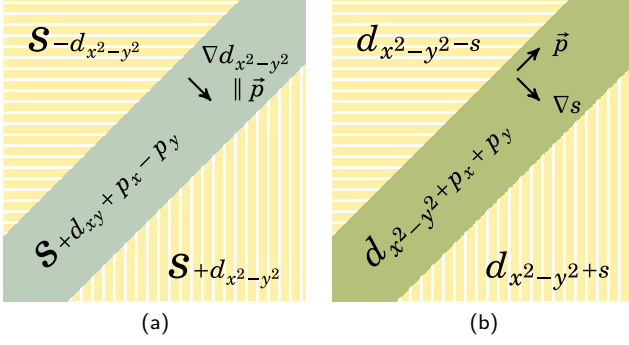


FIG. 1. Induced order parameter between two nematic domains. (a)  $(s \pm d)$  domain wall across which  $d_{x^2-y^2}$ -wave component changes sign. (b)  $(d \pm s)$  domain wall across which  $s$ -wave component changes sign. The induced  $p$ -wave component on the domain wall depends on which singlet order parameter changes sign.

eters in the corresponding channels. Since  $s$  is in the trivial  $A_1$  representation of  $C_{4v}$ , while both  $d_{x^2-y^2}$  and  $\eta$  are in the  $B_1$ , their product is trivial.

A domain wall between two nematic domains  $a > b$  and  $a < b$  forms a well-defined atomic junction when it is along the diagonal direction; it is indeed what is observed in FeSe [18] and also in other iron-pnictides in the nematic phase [16]. Under either  $C_4$  or  $\sigma_d$  symmetry operation  $d_{x^2-y^2}$ -wave component changes sign, while  $s$ -wave component is invariant. Therefore, the relative sign between the mixed  $s$ - and  $d_{x^2-y^2}$ -wave components flips across the domain wall. This change of relative sign between  $s$ - and  $d_{x^2-y^2}$ -component can manifest in two distinct ways: (1) the  $s$ -wave component stays constant or (2) the  $d$ -wave component stays constant across the domain wall. We refer to these two types of domain walls as  $(d \pm s)$  and  $(s \pm d)$ , respectively.

A so far little noted fact is that additional pairing components can be mixed in locally at the domain wall because of the lower symmetry of the domain wall. On a diagonal domain wall parallel to the  $[1\bar{1}0]$  plane as in Fig. 1, all the symmetry operations of  $C_{4v}$  are broken except  $\sigma_d(x-y)$ : the mirror reflection with respect to the  $[1\bar{1}0]$  plane [see Tab. I]. Since the component that remains finite at the domain wall behave distinctly under  $\sigma_d(x-y)$  for the  $(s \pm d)$  case [Fig. 1(a),  $s$  component is even] and the  $(d \pm s)$  case [Fig. 1(b),  $d_{x^2-y^2}$  component is odd], the new symmetry induced components also differ qualitatively for the two cases. Furthermore the SOC that is known to be substantial in FeSe [22–24] has unusual implications at the domain wall.

In the presence of the SOC,  $SU(2)$  spin-rotation symmetry is broken and singlets and triplets can mix in principle. However, when the SOC conserves  $S_z$ ,  $C_2$  symmetry still present within each nematic domains forbids mixing between singlets and triplets in the bulk of the

system. What has been overlooked so far is the fact that the domain wall itself lacks  $C_2$  symmetry and hence a  $S_z$  preserving SOC can couple  $p$ -wave components in the total  $S_z = 0$  channel with singlet components. This means the domain wall forms an emergent quasi-1D system with symmetry induced  $p$ -wave components.

Now we consider the  $(s \pm d)$  case and  $(d \pm s)$  case separately. For the  $(s \pm d)$  case [see Fig. 1(a)], the component that stays finite at the domain wall is  $s$ -wave, which is even under  $\sigma_d(x-y)$ . Now the lack of the  $C_2$  symmetry on the domain wall allows for  $d_{xy}$ , which is also even under  $\sigma_d(x-y)$ , to mix in. But most importantly a  $p$ -wave component perpendicular to the domain wall,  $(-p_x + p_y)$ -component, can be mixed in. One way to see this is to recognize that  $(-p_x + p_y)$  is also even under  $\sigma_d(x-y)$  since  $\sigma_d(x-y)$  affects both the spatial and spin coordinates of  $p$ -wave components. For instance,

$$p_x \sim c_{\hat{x},\uparrow} c_{-\hat{x},\downarrow} + c_{\hat{x},\downarrow} c_{-\hat{x},\uparrow}, \quad (2)$$

where  $\hat{x}$  is a spatial vector parallel to the  $x$ -axis transforms to  $-p_y$  under  $\sigma_d(x-y)$ . Similarly,  $p_y$  transforms to  $-p_x$ . Hence  $(-p_x + p_y)$  is even under  $\sigma_d(x-y)$ . Using the language of Ginzburg-Landau theory, the  $(s \pm d)$  domain wall imposes a gradient in the  $d_{x^2-y^2}$  component perpendicular to the domain wall, i.e.,  $\nabla d_{x^2-y^2} \propto (1, -1)$ . Since  $p_y$  transforms as  $-\hat{x}$  and  $p_x$  transforms as  $\hat{y}$ ,  $(p_y^* \partial_x + p_x^* \partial_y)$  transforms as  $B_1$  representation of  $C_{4v}$ . Hence the following coupling term is allowed by symmetry

$$\mathcal{L}_{s \pm d} = \gamma (p_y^* \partial_x + p_x^* \partial_y) d_{x^2-y^2} + \text{c.c.} \quad (3)$$

Now turning to the  $(d \pm s)$  case [Fig. 1(b)], the component that stays finite at the domain wall is now  $d_{x^2-y^2}$ , which is invariant under  $\sigma_d(x-y)$  followed by a gauge transformation by  $\pi$ . From Eq. (2),  $p_x + p_y$  is also invariant under the same discrete transformation and hence now a  $p$ -wave component along the domain wall is induced [see Fig. 1(b)]. From the GL theory perspective, it is the  $s$ -wave component that changes sign across the domain wall and hence the non-zero gradient is  $\nabla s \propto (1, -1)$ .  $(p_y^* \partial_x - p_x^* \partial_y)$  transforms as  $A_1$  representation, now the symmetry allowed coupling term is

$$\mathcal{L}_{d \pm s} = \gamma (p_y^* \partial_x - p_x^* \partial_y) s + \text{c.c.} \quad (4)$$

This implies that the gradient of  $s$ -wave component imposed by the domain wall in the dominantly  $d_{x^2-y^2}$ -wave nematic superconductor induces a  $p$ -wave component along the domain wall direction, defining an emergent 1D  $p$ -wave superconductor.

The above symmetry-based insights can be readily confirmed through an explicit microscopic calculation. For demonstration purpose, consider a two band toy model whose hopping is given in terms of operators  $c_{\alpha,\sigma}(\mathbf{r})$  which annihilate an electron at site  $\mathbf{r}$  with orbital  $\alpha = xz, yz$  and spin  $\sigma = \uparrow, \downarrow$  as

$$H_{\text{kinetic}}(\mathbf{r}, \mathbf{r}') = \mathbf{t}(\mathbf{r} - \mathbf{r}') \sigma_0 - \mu \delta_{\mathbf{r},\mathbf{r}'} \tau_0 \sigma_0 - \lambda \delta_{\mathbf{r},\mathbf{r}'} \tau_2 \sigma_3 \quad (5)$$

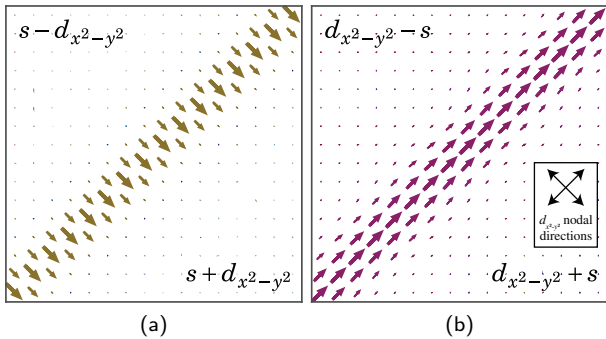


FIG. 2. Spatial distribution of pair amplitude in  $p$ -wave channel measured across a domain wall (a) when uniform  $s$ -wave pairing term is imposed, and (b) when uniform  $d_{x^2-y^2}$ -wave pairing is imposed. The direction of each arrow in (a) and (b) represent the direction of  $\mathbf{p}(\mathbf{r})$  component at each point as defined in Eq. (8). The inset of (b) shows the nodal directions of the  $d_{x^2-y^2}$ -wave component. Here we set  $\mu = 0.2$ ,  $\lambda = 1$ ,  $t_{xz,xz}(\hat{x}) = 1$ ,  $t_{xz,xz}(\hat{y}) = -0.5$ ,  $t_{xz,xz}(\hat{x} + \hat{y}) = t_{xz,yz}(\hat{x} + \hat{y}) = 0.2$ ,  $\Delta = 0.2$ , and  $\eta_0 = 0.2$ .

where  $\tau_i$  and  $\sigma_i$  for  $i = 0, 1, 2, 3$  are identity and Pauli matrices operating on orbital and spin spaces, respectively. Here,  $\mu$  and  $\lambda$  chemical potential, and spin-orbit coupling, and  $\mathbf{t}(\boldsymbol{\rho})$  is a matrix in orbital space which parametrizes hopping. In addition, we impose uniform singlet pairing of the dominant component for each domain wall configuration through

$$\mathcal{H}_{\text{pair}} = \Delta \sum_{\mathbf{r}} \sum_{\alpha=xz,yz} f_{\alpha} c_{\alpha,\uparrow}^{\dagger}(\mathbf{r}) c_{\alpha,\downarrow}^{\dagger}(\mathbf{r}) + \text{H.c.} \quad (6)$$

where  $f_{\alpha}$  is the orbital form factor:  $f_{\alpha} = f_{\alpha}^s \equiv 1$  for  $s$ -wave, and  $f_{\alpha} = f_{\alpha}^{d_{x^2-y^2}} \equiv [\tau_3]_{\alpha,\alpha}$  for  $d_{x^2-y^2}$ -wave. For  $(s \pm d)$  domain wall we impose a uniform  $s$ -wave pairing and for  $(d \pm s)$  domain wall we impose a uniform  $d_{x^2-y^2}$  pairing.

Now we impose a sharp nematic domain wall profile through an on-site orbital imbalance that changes sign across the domain wall, i.e.,

$$H_{\text{nematic}}(\mathbf{r}, \mathbf{r}') = \delta_{\mathbf{r},\mathbf{r}'} \eta(\mathbf{r}) \tau_3 \sigma_0. \quad (7)$$

where  $\eta(x, y) = \eta_0(2\Theta(x - y) - 1)$ . We then solve this mean-field theory to obtain the Bogoliubov eigenstates and measure the pair amplitudes on sites and nearest neighbor bonds with the obtained eigenstates. Without nematicity defined in Eq. (7), the measured pair amplitudes will trivially follow the symmetry of the imposed uniform pairing in Eq. (6). But the imposed nematic domain wall induces secondary components both in the domains as well as on the domain wall. In particular, plots of  $S_z = 0$  spin-triplet components defined by

$$\mathbf{p}(\mathbf{r}) = \sum_{\substack{\alpha=xz,yz \\ \boldsymbol{\rho}=\pm\hat{x},\pm\hat{y}}} \boldsymbol{\rho} (c_{\alpha,\uparrow}(\mathbf{r} + \boldsymbol{\rho}) c_{\alpha,\downarrow}(\mathbf{r}) + (\uparrow \leftrightarrow \downarrow)). \quad (8)$$

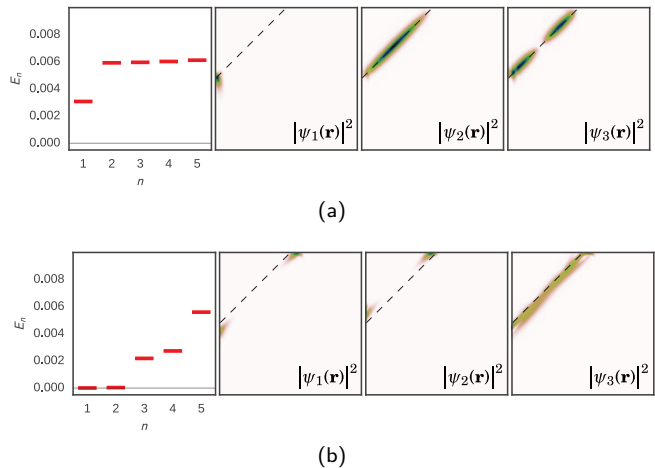


FIG. 3. Low lying eigenstates of a BdG Hamiltonian with a  $(d \pm s)$  domain wall for  $n$ 'th positive energy eigenstates (a) without  $p$ -wave component, and (b) with  $p$ -wave component at the domain wall. The spectra (the left most panels) and the spatial distribution of wave-function amplitudes  $|\psi_n(\mathbf{r})|^2$  of  $n = 1, 2$  and 3. The dashed lines indicate the location of the domain wall.

in Fig. 2(a) clearly shows  $p$ -wave components concentrated on the domain walls with its direction perpendicular to the domain wall for  $(s \pm d)$  case and parallel to the domain wall for  $(d \pm s)$  case. Interestingly, the  $(s \pm d)$  case can be viewed as two edges of  $d$ -wave superconductors brought close to each other. From this viewpoint, the induced  $p$ -wave perpendicular to the domain wall is a way a pair of flat-band zero modes predicted in Refs. [19, 20] pair up to gap out the low energy spectrum. Alternatively a large  $p$ -wave component parallel to the nematic domain wall can define an emergent one-dimensional topological superconductor for the  $(d \pm s)$  case. From the symmetry classification perspective [25], our system belongs to the DIII class with time reversal symmetry as in Ref. [26] with one difference being that our block Hamiltonians for each  $S_z$  blocks belong to AIII class. Hence the  $(d \pm s)$  opens possibility for zero energy Majorana bound states at the end of the “wire”.

To demonstrate the implication of the emergent  $p$ -wave wire on the  $(d \pm s)$  domain wall, we now consider a simple one-band Bogoliubov-de Gennes Hamiltonian. We consider two limits: when  $p$ -wave component is zero and when it is large. We work with a Bogoliubov-de Gennes Hamiltonian

$$H_{\mathbf{r},\mathbf{r}'} = \begin{pmatrix} t_{\mathbf{r},\mathbf{r}'} & \Delta_{\mathbf{r},\mathbf{r}'} \\ \Delta_{\mathbf{r}',\mathbf{r}}^* & -t_{\mathbf{r},\mathbf{r}'} \end{pmatrix}. \quad (9)$$

The hopping includes chemical potential and nearest neighbor hoppings  $t_{\mathbf{r},\mathbf{r}'} = -\mu\delta_{\mathbf{r},\mathbf{r}'} - t\delta_{(\mathbf{r},\mathbf{r}')}$ , with  $\mu = -3$  and  $t = 1$ . The imposed pairing is a superposition of uniform  $d_{x^2-y^2}$ -wave with domain-defining  $s$ -wave component (changing sign across the domain wall) and induced

$p$ -wave component local to the domain wall. The low energy spectra of the domain wall with and without the induced  $p$ -wave pairing differ qualitatively. Figures 3(a) and 3(b) show the energies of the low-lying single particle excitations near a  $(d \pm s)$  domain wall and their spatial profile, without and with the induced  $p$ -wave components, respectively. In both cases, we have set  $\Delta_d = 0.6$ ,  $\Delta_s = 0.4$ , and  $\xi = 8$ . The  $p$ -wave component  $\Delta_p$  is set to zero and 150 in Figs. 3(a) and 3(b), respectively. In the leftmost panels of Figs. 3(a) and 3(b), we plot positive the eigenenergies, since the product of time-reversal and particle-hole symmetry ensures that the eigenenergies come in  $(E, -E)$  pairs. Without the  $p$ -wave component on the domain wall, the excitation gap remains non-zero. When large  $p$ -wave component is introduced, on the other hand, energies of the first two eigen states drop to a value indistinguishable from zero within our calculation. These zero modes peak at  $\sim \xi$  away from the center of the domain wall on both of its sides, which account for the multiplicity of two for each spin state. Hence our domain wall supports four-channels of spinless  $p$ -wave wires.

Interestingly, the symmetry analysis we used here applies to a related situation of a clean edge of a  $d$ -wave superconductor [19, 20]. It was shown in Ref. [20] using quantum Monte Carlo simulations that ferromagnetic instability of Majorana flat band at a [110] edge of a  $d_{x^2-y^2}$  discussed by Potter and Lee [19] accompanies  $p$ -wave pairing along the edge. From the GL-theory perspective we have been using throughout this letter,

$$\mathcal{L}_{M-t} \propto M_z (p_x^* \partial_x - p_y^* \partial_y) d_{x^2-y^2} + c.c. \quad (10)$$

is a symmetry allowed term. This is because the magnetization order parameter  $M_z$  belongs to  $A_2$  representation while  $p_x^* \partial_x - p_y^* \partial_y$ , and  $d_{x^2-y^2}$  respectively falls into  $B_2$ , and  $B_1$  representations. Since the product is trivial, such a term is allowed and non-zero magnetization will be accompanied by  $p$ -wave pairing along the edge. This precedence of correspondence between exact numerical solution and our symmetry analysis lends further confidence to our predictions.

To summarize, we considered the problem of singlet-triplet mixing on a nematic domain wall in a superconductor with  $S_z$  preserving spin-orbit coupling with FeSe in mind. First we noted that  $C_2$  symmetry of each nematic domain requires the order parameter representation to be a mix of  $d$ -wave and  $s$ -wave component. Further lowering of symmetry on the domain wall allows for spin triplet components to mix in. We then noted that two distinct realizations of domain boundaries are possible depending on the dominant order parameter component. Specifically when the  $d$ -wave component is more dominant, the  $s$ -wave component changes sign across the domain wall ( $d \pm s$  domain wall) whereas when the  $s$ -wave component is more dominant the  $d$ -wave component changes sign across the domain wall ( $s \pm d$  domain

main wall). The two types of domain wall each support a locally induced spin-triplet  $p$ -wave components along different directions:  $p$ -wave along the wall direction for the  $(d \pm s)$  domain wall and  $p$ -wave perpendicular to the wall direction for the  $(s \pm d)$  domain wall. The  $p$ -wave component aligned parallel to the domain wall raises a tantalizing possibility of realizing a emergent 1D triplet superconductor with only four channels. Indeed our Bogoliubov-de Gennes calculation shows that such emergent 1D triplet superconductor will support Majorana zero-energy bound states. Given growing understanding of significance of  $d$ -component in FeSe [27–29], our findings call for further investigation of domain walls in FeSe and a search for Majorana zero modes at higher temperatures.

**Acknowledgements** We thank J.C. Davis, Jason Alicea, Rafael Fernandes, Piers Coleman, and Jian-Huang She for discussions. E-AK and KL were supported by the U.S. Department of Energy, Office of Basic Energy Sciences, Division of Materials Science and Engineering under Award DE-SC0010313. E-AK also acknowledges Simons Fellow in Theoretical Physics Award#392182 hospitality of the KITP supported by Grant No. NSF PHY11-25915. KL was supported in part by DOE Grant DE-FG02-07ER46423.

- 
- [1] V. Mourik, K. Zuo, S. M. Frolov, S. R. Plissard, E. P. A. M. Bakkers, and L. P. Kouwenhoven, “Signatures of Majorana fermions in hybrid superconductor-semiconductor nanowire devices,” *Science* **336**, 1003–1007 (2012).
  - [2] M. T. Deng, S. Vaitiekenas, E. B. Hansen, J. Danon, M. Leijnse, K. Flensberg, J. Nygård, P. Krogstrup, and C. M. Marcus, “Majorana bound state in a coupled quantum-dot hybrid-nanowire system,” *Science* **354**, 1557–1562 (2016).
  - [3] Stevan Nadj-Perge, Ilya K. Drozdov, Jian Li, Hua Chen, Sangjun Jeon, Jungpil Seo, Allan H. MacDonald, B. Andrei Bernevig, and Ali Yazdani, “Observation of Majorana fermions in ferromagnetic atomic chains on a superconductor,” *Science* **346**, 602–607 (2014).
  - [4] Jason Alicea, “New directions in the pursuit of majorana fermions in solid state systems,” *Reports on Progress in Physics* **75**, 076501 (2012).
  - [5] Shuichi Murakami, “Phase transition between the quantum spin Hall and insulator phases in 3D: Emergence of a topological gapless phase,” *New J. Phys.* **9**, 356 (2007).
  - [6] Xiangang Wan, Ari M. Turner, Ashvin Vishwanath, and Sergey Y. Savrasov, “Topological semimetal and Fermi-arc surface states in the electronic structure of pyrochlore iridates,” *Phys. Rev. B* **83**, 205101 (2011).
  - [7] Mitsutaka Fujita, Katsunori Wakabayashi, Kyoko Nakada, and Koichi Kusakabe, “Peculiar localized state at zigzag graphite edge,” *J. Phys. Soc. Jpn.* **65**, 1920–1923 (1996).

- [8] Chia-Ren Hu, “Midgap surface states as a novel signature for  $d_{x_a^2-x_b^2}$ -wave superconductivity,” *Phys. Rev. Lett.* **72**, 1526–1529 (1994).
- [9] Fa Wang and Dung-Hai Lee, “Topological relation between bulk gap nodes and surface bound states: Application to iron-based superconductors,” *Phys. Rev. B* **86**, 094512 (2012).
- [10] Eduardo Fradkin, Steven A. Kivelson, and John M. Tranquada, “*Colloquium*: Theory of intertwined orders in high temperature superconductors,” *Rev. Mod. Phys.* **87**, 457–482 (2015).
- [11] R. M. Fernandes, A. V. Chubukov, and J. Schmalian, “What drives nematic order in iron-based superconductors?” *Nature Phys.* **10**, 97–104 (2014).
- [12] Jiun-Haw Chu, James G. Analytis, Kristiaan De Greve, Peter L. McMahon, Zahirul Islam, Yoshihisa Yamamoto, and Ian R. Fisher, “In-plane resistivity anisotropy in an underdoped iron arsenide superconductor,” *Science* **329**, 824–826 (2010).
- [13] T.-M. Chuang, M. P. Allan, Jinho Lee, Yang Xie, Ni Ni, S. L. Bud’ko, G. S. Boebinger, P. C. Canfield, and J. C. Davis, “Nematic electronic structure in the “parent” state of the iron-based superconductor  $\text{Ca}(\text{Fe}_{1-x}\text{Co}_x)_2\text{As}_2$ ,” *Science* **327**, 181–184 (2010).
- [14] Qing-Yan Wang, Zhi Li, Wen-Hao Zhang, Zuo-Cheng Zhang, Jin-Song Zhang, Wei Li, Hao Ding, Yun-Bo Ou, Peng Deng, Kai Chang, Jing Wen, Can-Li Song, Ke He, Jin-Feng Jia, Shuai-Hua Ji, Ya-Yu Wang, Li-Li Wang, Xi Chen, Xu-Cun Ma, and Qi-Kun Xue, “Interface-induced high-temperature superconductivity in single unit-cell FeSe films on  $\text{SrTiO}_3$ ,” *Chin. Phys. Lett.* **29**, 037402 (2012).
- [15] Defa Liu, Wenhao Zhang, Daixiang Mou, Junfeng He, Yun-Bo Ou, Qing-Yan Wang, Zhi Li, Lili Wang, Lin Zhao, Shaolong He, Yingying Peng, Xu Liu, Chaoyu Chen, Li Yu, Guodong Liu, Xiaoli Dong, Jun Zhang, Chuangtian Chen, Zuyan Xu, Jiangping Hu, Xi Chen, Xucun Ma, Qikun Xue, and X.J. Zhou, “Electronic origin of high-temperature superconductivity in single-layer FeSe superconductor,” *Nature Comm.* **3**, 931– (2012).
- [16] B. Kalisky, J. R. Kirtley, J. G. Analytis, Jiun-Haw Chu, A. Vaillonis, I. R. Fisher, and K. A. Moler, “Stripes of increased diamagnetic susceptibility in underdoped superconducting  $\text{Ba}(\text{Fe}_{1-x}\text{Co}_x)_2\text{As}_2$  single crystals: Evidence for an enhanced superfluid density at twin boundaries,” *Phys. Rev. B* **81**, 184513 (2010).
- [17] Can-Li Song, Yi-Lin Wang, Peng Cheng, Ye-Ping Jiang, Wei Li, Tong Zhang, Zhi Li, Ke He, Lili Wang, Jin-Feng Jia, Hsiang-Hsuan Hung, Congjun Wu, Xucun Ma, Xi Chen, and Qi-Kun Xue, “Direct observation of nodes and twofold symmetry in FeSe superconductor,” *Science* **332**, 1410–1413 (2011).
- [18] T. Watashige, Y. Tsutsumi, T. Hanaguri, Y. Kohsaka, S. Kasahara, A. Furusaki, M. Sigrist, C. Meingast, T. Wolf, H. v. Löhneysen, T. Shibauchi, and Y. Matsuda, “Evidence for time-reversal symmetry breaking of the superconducting state near twin-boundary interfaces in FeSe revealed by scanning tunneling spectroscopy,” *Phys. Rev. X* **5**, 031022 (2015).
- [19] Andrew C. Potter and Patrick A. Lee, “Edge ferromagnetism from Majorana flat bands: Application to split tunneling-conductance peaks in high- $T_c$  cuprate superconductors,” *Phys. Rev. Lett.* **112**, 117002 (2014).
- [20] Johannes S. Hofmann, Fakher F. Assaad, and Andreas P. Schnyder, “Edge instabilities of topological superconductors,” *Phys. Rev. B* **93**, 201116 (2016).
- [21] G. R. Stewart, “Superconductivity in iron compounds,” *Rev. Mod. Phys.* **83**, 1589–1652 (2011).
- [22] S. V. Borisenko, D. V. Evtushinsky, Z.-H. Liu, I. Morozov, R. Kappenberger, S. Wurmehl, B. Buchner, A. N. Yaresko, T. K. Kim, M. Hoesch, T. Wolf, and N. D. Zhigadlo, “Direct observation of spin-orbit coupling in iron-based superconductors,” *Nature Phys.* **12**, 311–317 (2016).
- [23] M. Ma, P. Bourges, Y. Sidis, Y. Xu, S. Li, B. Hu, J. Li, F. Wang, and Y. Li, “Prominent role of spin-orbit coupling in FeSe,” ArXiv e-prints (2016), [arXiv:1610.01277](https://arxiv.org/abs/1610.01277) [[cond-mat.supr-con](https://arxiv.org/archive/cond-mat)].
- [24] Vladimir Cvetkovic and Oskar Vafek, “Space group symmetry, spin-orbit coupling, and the low-energy effective Hamiltonian for iron-based superconductors,” *Phys. Rev. B* **88**, 134510 (2013).
- [25] Andreas P. Schnyder, Shinsei Ryu, Akira Furusaki, and Andreas W. W. Ludwig, “Classification of topological insulators and superconductors in three spatial dimensions,” *Phys. Rev. B* **78**, 195125 (2008).
- [26] Jan Carl Budich and Eddy Ardonne, “Topological invariant for generic one-dimensional time-reversal-symmetric superconductors in class DIII,” *Phys. Rev. B* **88**, 134523 (2013).
- [27] J.-H. She, M. J. Lawler, and E.-A. Kim, “Mechanism for nematic superconductivity in FeSe,” ArXiv e-prints (2017), [arXiv:1701.07813](https://arxiv.org/abs/1701.07813) [[cond-mat.str-el](https://arxiv.org/archive/cond-mat)].
- [28] Shantanu Mukherjee, A. Kreisel, P. J. Hirschfeld, and Brian M. Andersen, “Model of electronic structure and superconductivity in orbitally ordered FeSe,” *Phys. Rev. Lett.* **115**, 026402 (2015).
- [29] P. O. Sprau, A. Kostin, A. Kreisel, A. E. Böhmer, V. Taufour, P. C. Canfield, S. Mukherjee, P. J. Hirschfeld, B. M. Andersen, and J. C. Séamus Davis, “Discovery of orbital-selective Cooper pairing in FeSe,” ArXiv e-prints (2016), [arXiv:1611.02134](https://arxiv.org/abs/1611.02134) [[cond-mat.supr-con](https://arxiv.org/archive/cond-mat)].